Earthq Sci (2016) 29(5):291–298
DOI 10.1007/s11589-016-0167-y

RESEARCH PAPER

Long aseismic slip duration of the 2006 Java tsunami earthquake based on GPS data

Rio Raharja · Endra Gunawan · Irwan Meilano · Hasanuddin Z. Abidin · Joni Efendi

Received: 5 April 2016 / Accepted: 12 September 2016 / Published online: 21 October 2016

Abstract The Java earthquake occurred on July 17, 2006 with magnitude 7.8 associated to the subduction process of Indo-Australian plate and Sundaland block off southwestern coast of Java. We present postseismic deformation parameters of the 2006 Java earthquake analyzed using campaign GPS observation from 2006 to 2008 and continuous observation from 2007 to 2014. We use an analytical approach of logarithmic and exponential functions to model these GPS data. We find that the decay time in the order of hundreds of days after the mainshock as observed by 8 years' data after the mainshock for magnitude 7 earthquake is longer than a general megathrust earthquake event. Our findings suggest that the 2006 Java earthquake which is considered as "tsunami earthquake" most probably occurred in the region that has low rigidity and tends to continuously slip for long time periods.

Keywords 2006 Java earthquake · Aseismic slip · GPS · Time series

R. Raharja (✉) · I. Meilano · H. Z. Abidin
Geodesy and Geomatics Engineering, Faculty of Earth Sciences and Technology, Bandung Institute of Technology, Bandung, Indonesia
e-mail: rio.raharja@students.itb.ac.id

E. Gunawan · I. Meilano
Graduate Research on Earthquake and Active Tectonics, Faculty of Earth Sciences and Technology, Bandung Institute of Technology, Bandung, Indonesia

J. Efendi
Geospatial Information Agency of Indonesia, Cibinong, Indonesia

1 Introduction

The subduction process of Indo-Australian plate toward Sundaland block in the southern Java, Indonesia, suggests that this is a tectonically active region and prone to earthquake occurrences (Richards et al. 2007). One of the events is the 2006 *M*7.8 Java earthquake, which occurred on July 17, 2006 at 08:19 UTC (Fig. 1). This earthquake produced a devastating tsunami up to 7 m that caused casualties of more than 600 people and more than 50,000 people lost their houses (Kato et al. 2007).

Soon after the mainshock, campaign Global Positioning System (GPS) measurements were taken near the source region by Geodesy Research Division of Bandung Institute of Technology (ITB) along the southern coast of western Java (Abidin et al. 2009). The campaign observation from 2006 to 2008 showed a significant signal of postseismic deformation after the earthquake. Using continuous GPS data from Geospatial Information Agency of Indonesia (BIG) during the time period of 2008–2010, Hanifa et al. (2014) analyzed postseismic deformation associated to afterslip using these continuous GPS datasets. Other study suggested that postseismic deformation associated to viscoelastic relaxation should also take into account for the 2006 Java earthquake (Gunawan et al. 2016).

This study analyzed postseismic deformation parameters of the 2006 Java earthquake using all available GPS datasets obtained from campaign observation from 2006 to 2008 and continuous observation from 2007 to 2014. Table 1 shows the description of GPS stations of this study. The early campaign GPS data are very important because they captured early postseismic deformation signal (Ito et al. 2012). Unfortunately, previous studies have never analyzed these early campaign data. The newly available

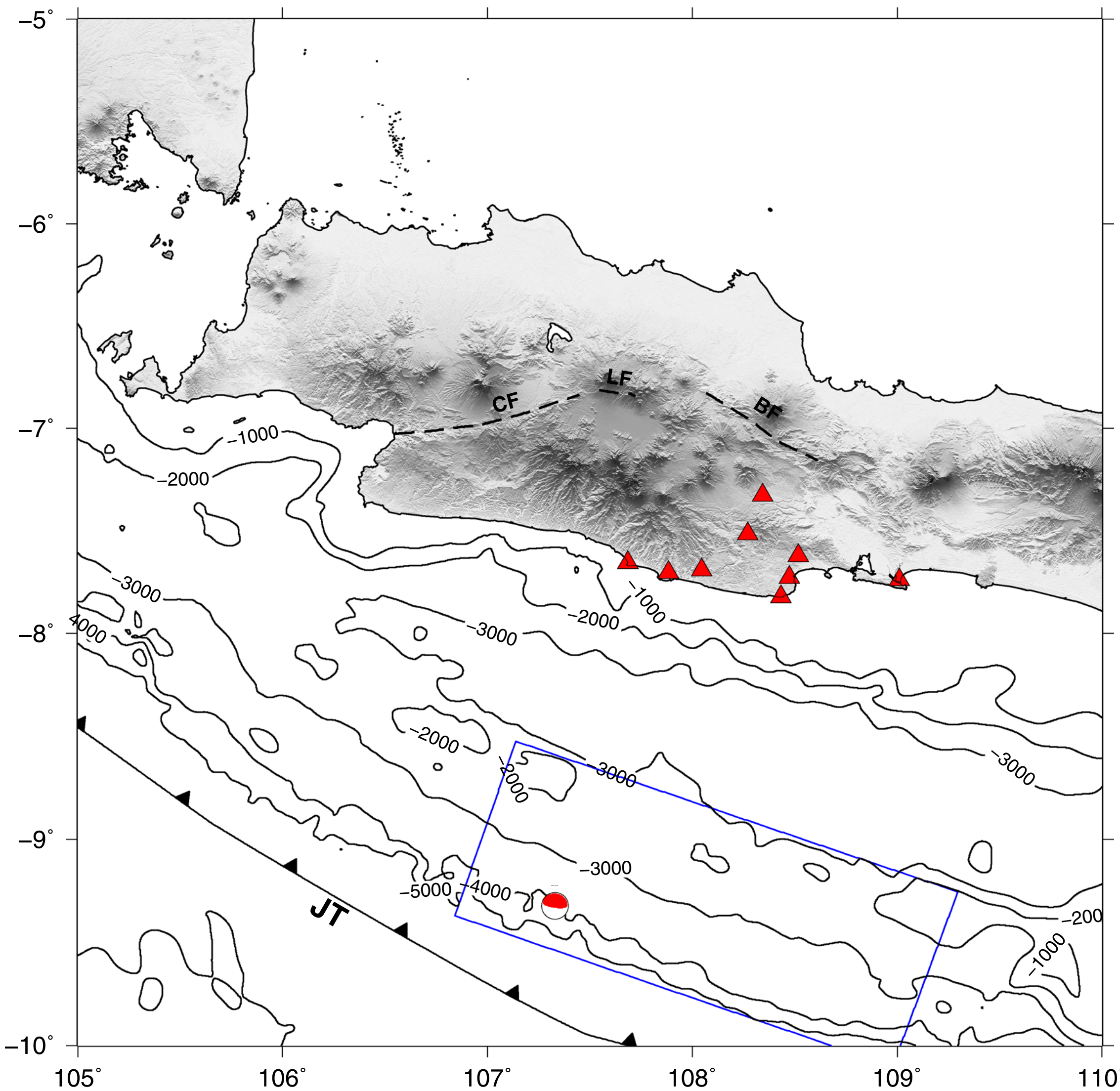

Fig. 1 Overview of tectonics condition in the study area. *Dashed black lines* indicate inland faults. *Red triangles* imply GPS stations used in this study. Beachball shows the epicenter location of the 2006 Java earthquake and the coseismic fault rupture is denoted by *blue box*, based on Bilek and Engdahl (2007). *JT* Java trench, *CF* Cimandiri fault, *LF* Lembang fault, *BF* Baribis fault. Seabed contours derived from ETOPO 1 (Amante and Eakins 2009)

Table 1 Description of GPS stations of this study

Station	Long. (°E)	Lat. (°S)	Type	Institution	Data availability
0448	108.2713	7.5142	Campaign	ITB	2006–2008
0452	107.8828	7.7018	Campaign	ITB	2006–2008
0455	108.0453	7.6906	Campaign	ITB	2006–2008
0461	108.5175	7.6205	Campaign	ITB	2006–2008
0465	108.4725	7.7273	Campaign	ITB	2006–2008
LGJW	108.4318	7.8205	Campaign	ITB	2006–2008
CCLP	109.0102	7.7376	Continuous	BIG	2010–2014
CMIS	108.3434	7.3261	Continuous	BIG	2010–2014
CPMK	107.6905	7.6551	Continuous	BIG	2007–2012

continuous GPS data used in our analysis have never been used by previous study, which only analyzed continuous GPS data until 2010. Using these newly available GPS datasets, we analyzed the characteristics of postseismic deformation after the 2006 Java using analytical approach of logarithmic and exponential functions.

2 Data and method

In this study, we use two types of GPS datasets obtained from campaign and continuous observations, respectively. Abidin et al. (2009) reported campaign GPS observations during the time period of 2006–2008. In total, there are 30 GPS stations located along the southern coast of western Java. Unfortunately, among these 30 stations, only 6 stations were revisited continuously every year from 2006 to 2008. Most of these stations were only revisited two times during 2006–2007, or during 2007–2008. In this study, we use these 6 stations for further postseismic deformation analysis.

In addition to these campaign GPS data, we also use continuous GPS data installed and maintained by BIG in western Java. In this study, we use 3 GPS stations with continuous data available from 2007 to 2014. Figure 2 shows the distribution of GPS stations used in this study.

We analyzed these GPS data and obtained daily solutions using scientific software GAMIT/GLOBK (Herring et al. 2010a, b). During the analysis, we fix the preliminary coordinate results of ten International GNSS Service (IGS) stations to obtain daily solutions in International Terrestrial Reference Frame (ITRF) 2008. These IGS stations include COCO, CNMR, DARW, DGAR, HYDE, IISC, KARR, PIMO, TOW2, and TNML. The daily solutions were then transformed into ITRF2000 reference frame (Altamimi et al. 2011) and recalculated relative to Sundaland block reference frame using transformation parameters of rotation pole as follows: 49.0°N, −94.2°E, 0.336°/Ma (Simons et al. 2007). Figure 3 shows the time series of GPS data used in this study.

In the next analysis procedure, we modeled GPS time series displacements using the logarithmic function of Marone et al. (1991) and the exponential function of Savage and Prescott (1978). In these equations, t corresponds to time since earthquake, $u(t)$ is the displacement in north and east components, c is the data offset, τ_{log} and τ_{exp} are the decay times in logarithmic and exponential functions, respectively, and a is the amplitude associated with the decay.

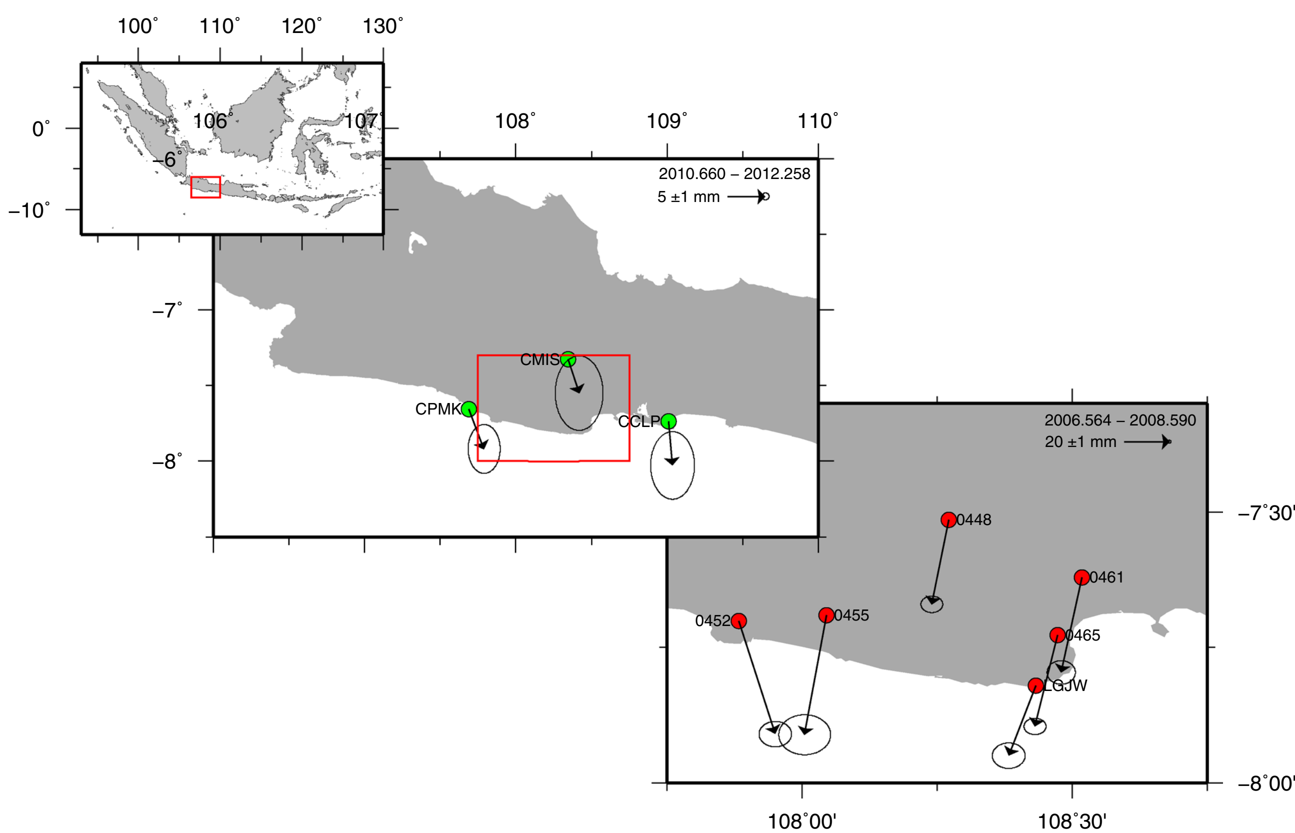

Fig. 2 GPS displacements with reference to Sundaland block at continuous and campaign GPS stations indicated by *green circles* and *red circles*

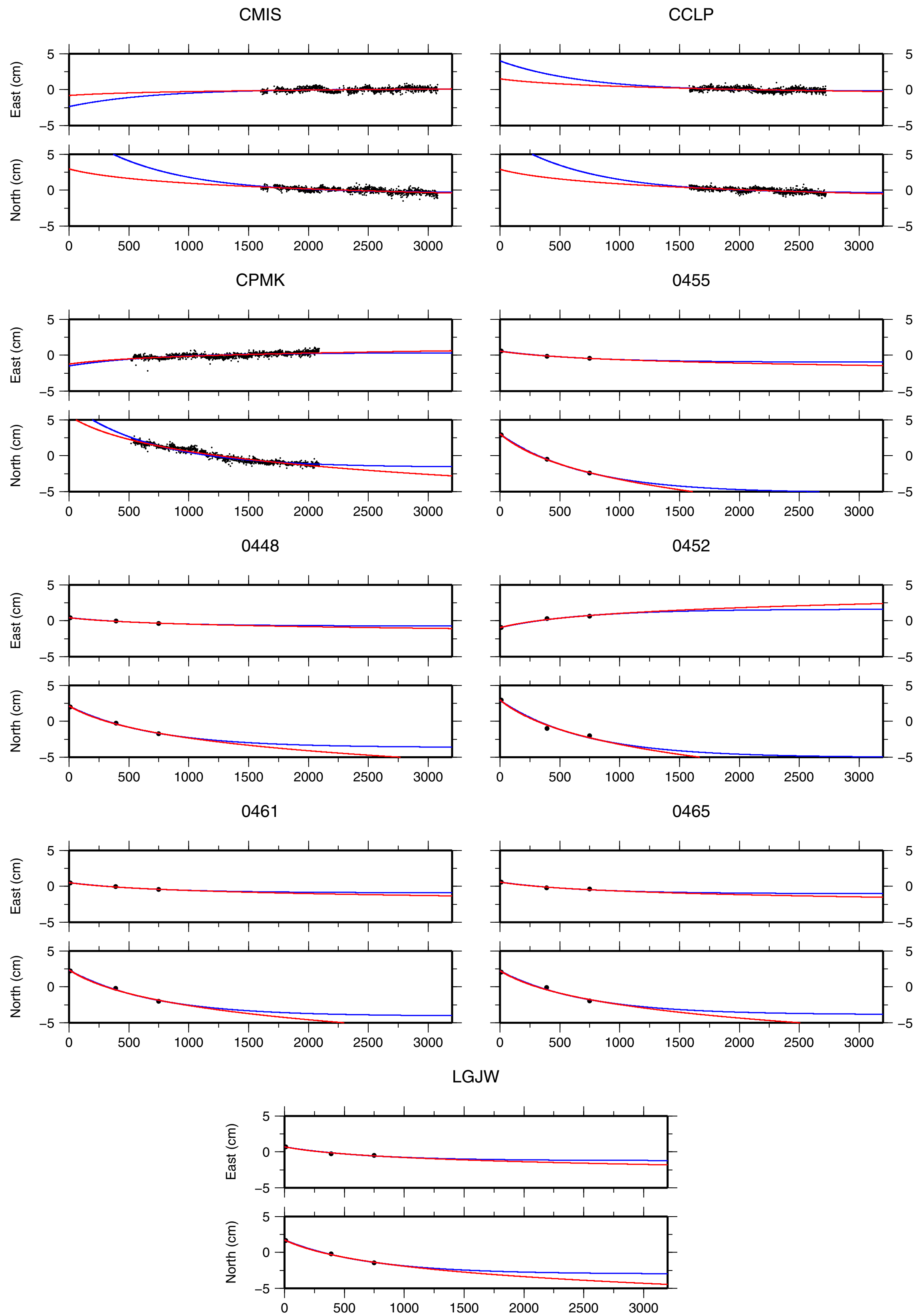

Fig. 3 Time series of GPS data used in this study. Red line indicates the best fit of logarithmic function, while *blue* line implies the best fit of exponential function

3 Modeling results

During the time period of 2006–2008, GPS stations along the southern coast of western Java moved toward the rupture area of the 2006 Java earthquake, consistent with the motion of the coseismic rupture suggesting the occurrence of postseismic deformation during this time period (Ito et al. 2016). Further analysis using continuous GPS data from 2008 to 2010 also suggested the ongoing postseismic deformation in this region (Gunawan et al. 2016). Using different datasets to Gunawan et al. (2016) and include data in a longer time period until 2014, we show that postseismic deformation of the 2006 Java earthquake area is still continuing (Fig. 2).

We applied the logarithmic and exponential mathematical functions to model the GPS time series, the unknown parameters a, c, $\tau_{\log}$, and $\tau_{\exp}$ are calculated using least square approach. In the first step, we vary $\tau_{\log}$ and $\tau_{\exp}$ in the range of 480–500 and 860–880 days for every 0.1-day step. For each $\tau_{\log}$ and $\tau_{\exp}$, we calculated a and c. During the search of best-fit parameters, we found that the decay time obtained for logarithmic function, $\tau_{\log}$, is 488.0 ± 0.1 days, while that for exponential function, $\tau_{\exp}$, is 871.0 ± 0.1 days (Fig. 4). Our analysis was performed using the data interval of 0.1 days, and each GPS station has different values of a and c, both in logarithmic and exponential functions. Table 2 shows the best-fit postseismic deformation parameters with minimum standard deviations for logarithmic function at each GPS station, while the best-fit parameters for exponential function are listed in Table 3.

4 Discussion

Our results suggest that the fits to the data using logarithmic and exponential functions are similar. As shown in Tables 2 and 3, there were only small differences between RMS results, as a result of the sensitivity of the availability of early GPS data just after earthquake occurrences to the logarithmic and exponential functions. As reported for other earthquake cases, such as the 2004 *M*9.2 Sumatra-Andaman earthquake (Anugrah et al. 2015), the 2005 *M*8.7 Nias earthquake (Kreemer et al. 2006), the 2007 *M*8.5 Bengkulu earthquake (Alif et al. 2016), and the 2010 *M*7.8 Mentawai earthquake (Ardika et al. 2015), they obtained a better data fit using logarithmic function for the early postseismic GPS data.

In the case of the 2006 Java earthquake, such early continuous GPS data are not available. The continuous GPS data in western Java are only available 2 years after the earthquake. On the other hand, the campaign GPS data were only measured once per year from 2006 to 2008. With this type of campaign GPS data, we cannot capture early postseismic deformation after the 2006 Java earthquake comprehensively. Hence, continuous GPS data soon after earthquake are very important for crustal deformation studies.

The decay time of postseismic deformation result suggests that the afterslip decay time of the 2006 Java earthquake is in the order of hundreds of days. This is much longer than that for a general megathrust earthquake (Bürgmann et al. 2001; Freed 2007; Anugrah et al. 2015). Those analyses showed that for an *M*6–8 class earthquake,

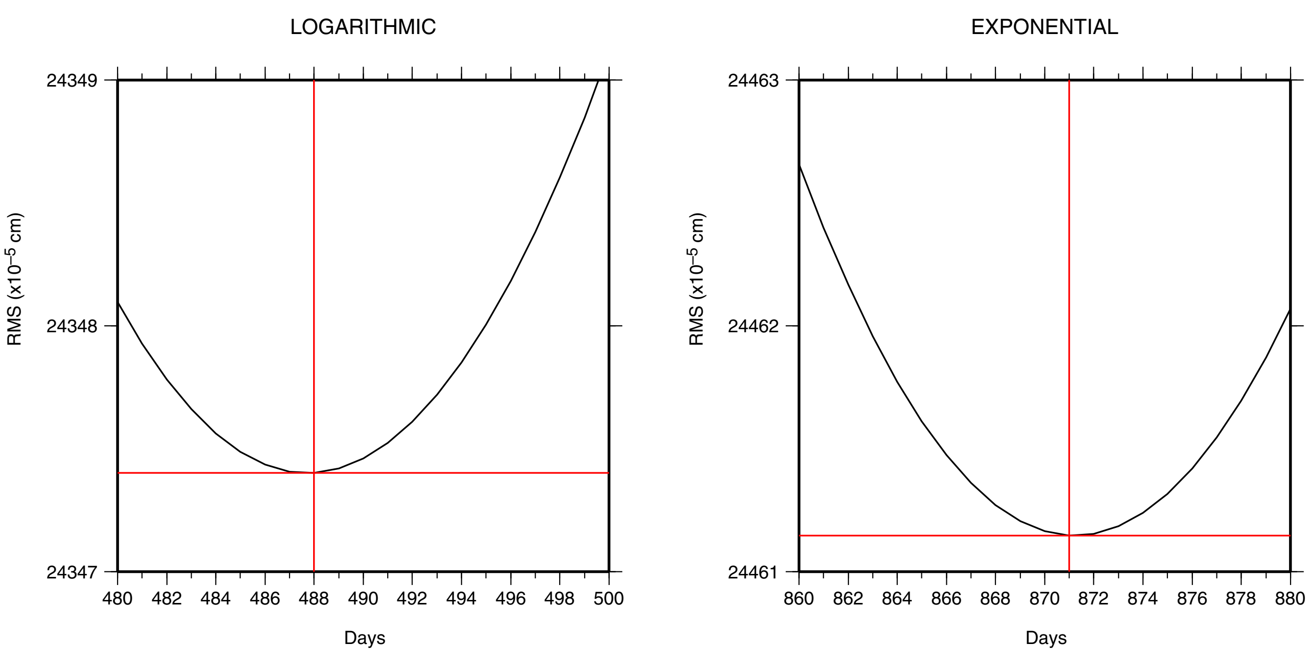

Fig. 4 Best-fit calculated decay time for (*left*) logarithmic function and (*right*) exponential function

Table 2 Best-fit postseismic deformation parameters calculated in logarithmic function

Stations	*c*		*a*		RMS
	N (cm)	E (cm)	N (cm)	E (cm)	
CCLP	4.59 ± 0.06	−3.62 ± 0.10	−1.52 ± 0.05	−0.79 ± 0.06	0.33
CPMK	7.00 ± 0.02	−6.62 ± 0.03	−3.90 ± 0.03	0.87 ± 0.02	0.36
CMIS	4.56 ± 0.05	−5.91 ± 0.08	−1.49 ± 0.05	0.41 ± 0.05	0.35
0455	3.94 ± 0.07	−1.99 ± 0.05	−5.81 ± 0.08	−1.09 ± 0.07	0.08
0448	3.06 ± 0.04	−2.13 ± 0.02	−4.09 ± 0.03	−0.82 ± 0.04	0.04
0452	3.84 ± 0.19	−3.48 ± 0.12	−5.62 ± 0.64	1.81 ± 0.19	0.53
0461	3.03 ± 0.03	−2.04 ± 0.02	−4.57 ± 0.14	−1.01 ± 0.03	0.11
0465	3.18 ± 0.15	−1.96 ± 0.09	−4.34 ± 0.27	−1.14 ± 0.14	0.25
LGJW	2.69 ± 0.17	−1.85 ± 0.11	−3.37 ± 0.05	−1.35 ± 0.17	0.14
Average					0.24

Table 3 Best-fit postseismic deformation parameters calculated in exponential function

Stations	*c*		*a*		RMS
	N (cm)	E (cm)	N (cm)	E (cm)	
CCLP	1.56 ± 0.08	−5.21 ± 0.01	−6.12 ± 0.21	−3.25 ± 0.22	0.33
CPMK	0.14 ± 0.02	−5.12 ± 0.00	−8.17 ± 0.05	1.73 ± 0.05	0.36
CMIS	1.51 ± 0.01	−5.08 ± 0.00	−6.84 ± 0.21	1.84 ± 0.21	0.36
0455	−5.06 ± 0.09	−3.68 ± 0.07	−8.99 ± 0.15	−1.69 ± 0.12	0.10
0448	−3.27 ± 0.05	−3.41 ± 0.04	−6.33 ± 0.03	−1.27 ± 0.06	0.03
0452	−4.87 ± 1.01	−0.67 ± 0.73	−8.70 ± 1.05	2.80 ± 0.31	0.54
0461	−3.77 ± 0.19	−3.59 ± 0.14	−7.07 ± 0.19	−1.55 ± 0.04	0.10
0465	−3.54 ± 0.34	−3.72 ± 0.25	−6.72 ± 0.42	−1.76 ± 0.24	0.24
LGJW	−2.52 ± 0.28	−3.95 ± 0.20	−5.21 ± 0.07	−2.10 ± 0.29	0.15
Average					0.25

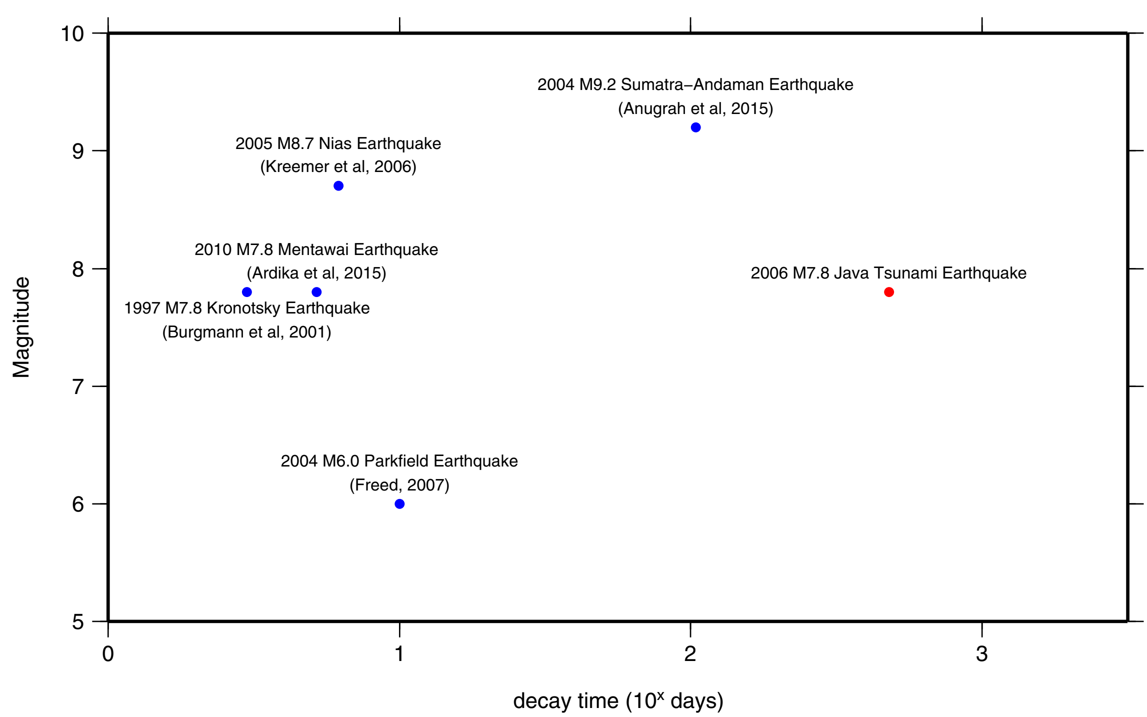

Fig. 5 Correlation between decay time after earthquake occurrences and earthquake magnitude for various earthquake cases

the decay time value is ~10 days. Our decay time of 488 days suggests that the 2006 Java earthquake is much longer than those earthquake cases, even for the *M*9 class earthquake (Fig. 5).

As suggested in a previous study (Ammon et al. 2006), the 2006 Java earthquake was considered as "tsunami earthquake" based on the characteristics of its long rupture duration (Bilek and Engdahl 2007), low rupture velocity (Kato et al. 2007), and the coseismic slip that occurred on shallow parts of the fault (Fujii and Satake 2006). In addition to those studies, our result of long decay postseismic deformation time supports the characteristic of a "tsunami earthquake." Our results of long decay time after the 2006 Java earthquake strongly suggest that the southwestern Java regions have lower rigidity than general megathrust earthquake cases and tend to continuously slip during long-term periods as a result of stress transfer from the mainshock (Polet and Kanamori 2000).

Our results regarding decay time in the order of hundreds of days as observed by 8 years' data after the event suggest that other physical mechanisms of postseismic deformations should be taken into account (Gunawan et al. 2014). In a much longer time period, the contribution of viscoelastic relaxation in the asthenosphere becomes compulsory as afterslip tends to decrease with time. Using an analytical approach of logarithmic and exponential functions, we showed that postseismic deformation parameters can be analyzed comprehensively.

5 Conclusions

In this study, we showed that we can fit campaign and continuous GPS data in western Java, Indonesia, using logarithmic and exponential functions. Similarities of misfit from two different functions suggest the importance of GPS data availability just after earthquake occurrences for crustal deformation analysis. Our results on postseismic deformation decay time indicate that it is in the order of 100 days after the mainshock. These findings suggest the 2006 Java earthquake be considered as a "tsunami earthquake" where the regions have low rigidity and tend to continuously slip for long time periods.

Acknowledgments We thank the reviewers and the editor for their thoughtful comments and constructive suggestions which help improve the quality of this manuscript. This research was partially supported by the Australian Department of Foreign Affairs and Trade (DFAT) for Graduate Research on Earthquake and Active Tectonics at the Bandung Institute of Technology and Research Program of Bandung Institute of Technology No. FITB.PN-06-01-2016. The figures were generated using GMT software (Wessel and Smith 1998).

References

Abidin HZ, Andreas H, Kato T, Ito T, Meilano I, Kimata F, Natawidjaya DH, Harjono H (2009) Crustal deformation studies in Java (Indonesia) using GPS. J Earthq Tsunami 3(02):77–88

Alif SM, Meilano I, Gunawan E, Efendi J (2016) Evidence of postseismic deformation signal of the 2007 *M*8. 5 Bengkulu earthquake and the 2012 *M*8. 6 Indian Ocean Earthquake in Southern Sumatra, Indonesia, based on GPS data. J Appl Geod 10(2):103–108. doi:10.1515/jag-2015-0019

Altamimi Z, Collilieux X, Métivier L (2011) ITRF2008: an improved solution of the international terrestrial reference frame. J Geod 85(8):457–473

Amante C, Eakins BW (2009) ETOPO1 1 arc-minute global relief model: procedures, data sources and analysis. US Department of Commerce, National Oceanic and Atmospheric Administration, National Environmental Satellite, Data, and Information Service, National Geophysical Data Center, Marine Geology and Geophysics Division, p 19

Ammon CJ, Kanamori H, Lay T, Velasco AA (2006) The 17 July 2006 Java tsunami earthquake. Geophys Res Lett. doi:10.1029/2006GL028005

Anugrah B, Meilano I, Gunawan E, Efendi J (2015) Estimation of postseismic deformation parameters from continuous GPS data in northern Sumatra after the 2004 Sumatra-Andaman earthquake. Earthq Sci 28(5–6):347–352. doi:10.1007/s11589-015-0136-x

Ardika M, Meilano I, Gunawan E (2015) Postseismic deformation parameters of the 2010 *M*7.8 Mentawai, Indonesia, earthquake inferred from continuous GPS observations. Asian J Earth Sci 8:127–133. doi:10.3923/ajes.2015.127.133

Bilek SL, Engdahl ER (2007) Rupture characterization and aftershock relocations for the 1994 and 2006 tsunami earthquakes in the Java subduction zone. Geophys Res Lett 34:L20311. doi:10.1029/2007GL031357

Bürgmann R, Kogan MG, Levin VE, Scholz CH, King RW, Steblov GM (2001) Rapid aseismic moment release following the 5 December, 1997 Kronotsky, Kamchatka, earthquake. Geophys Res Lett 28(7):1331–1334

Freed AM (2007) Afterslip (and only afterslip) following the 2004 Parkfield, California, earthquake. Geophys Res Lett. doi:10.1029/2006GL029155

Fujii Y, Satake K (2006) Source of the July 2006 West Java tsunami estimated from tide gauge records. Geophys Res Lett. doi:10.1029/2006GL028049

Gunawan E, Sagiya T, Ito T, Kimata F, Tabei T, Ohta Y, Meilano I, Abidin HZ, Agustan, Nurdin I, Sugiyanto D (2014) A comprehensive model of postseismic deformation of the 2004 Sumatra-Andaman earthquake deduced from GPS observations in northern Sumatra. J Asian Earth Sci 88:218–229. doi:10.1016/j.jseaes.2014.03.016

Gunawan E, Meilano I, Abidin HZ, Hanifa NR, Susilo (2016) Investigation of the best coseismic fault model of the 2006 Java tsunami earthquake based on mechanisms of postseismic deformation. J Asian Earth Sci 117:64–72. doi:10.1016/j.jseaes.2015.12.003

Hanifa NR, Sagiya T, Kimata F, Efendi J, Abidin HZ, Meilano I (2014) Interplate coupling model off the southwestern coast of Java, Indonesia, based on continuous GPS data in 2008–2010. Earth Planet Sci Lett 401:159–171

Herring TA, King RW, McClusky SC (2010a) GAMIT Reference Manual Release 10.4. Report, Massachussetts Institute Technology, Cambridge, pp 1–171

Herring TA, King RW, McClusky SC (2010b) GLOBK Reference Manual: Global Kalman filter VLBI and GPS analysis program, Release 10.4. Report, Massachussetts Institute Technology, Cambridge, pp 1–95

Ito T, Gunawan E, Kimata F, Tabei T, Simons M, Meilano I, Agustan, Ohta Y, Nurdin I, Sugiyanto D (2012) Isolating along-strike variations in the depth extent of shallow creep and fault locking on the northern Great Sumatran Fault. J Geophys Res: Solid Earth (1978–2012) 117(B6)

Ito T, Gunawan E, Kimata F, Tabei T, Meilano I, Agustan, Ohta YA, Ismail N, Nurdin I, Sugiyanto D (2016) Co-seismic offsets due to two earthquakes (M_W6.1) along the Sumatran fault system derived from GNSS measurements. Earth Planets Space 68:57. doi:10.1186/s40623-016-0427-z

Kato T, Ito T, Abidin HZ, Agustan (2007) Preliminary report on crustal deformation surveys and tsunami measurements caused by the July 17, 2006 South off Java Island Earthquake and Tsunami, Indonesia. Earth Planets Space 59(9):1055–1059

Kreemer C, Blewitt G, Maerten F (2006) Co-and postseismic deformation of the 28 March 2005 Nias M_W 8.7 earthquake from continuous GPS data. Geophys Res Lett 33(7):L07307

Marone CJ, Scholtz CH, Bilham R (1991) On the mechanics of earthquake afterslip. J Geophys Res: Solid Earth (1978–2012) 96(B5):8441–8452

Polet J, Kanamori H (2000) Shallow subduction zone earthquakes and their tsunamigenic potential. Geophys J Int 142(3):684–702

Richards S, Lister G, Kennett B (2007) A slab in depth: three-dimensional geometry and evolution of the Indo-Australian plate. Geochem Geophys Geosyst. doi:10.1029/2007GC001657

Savage JC, Prescott WH (1978) Asthenosphere readjustment and the earthquake cycle. J Geophys Res: Solid Earth (1978–2012) 83(B7):3369–3376

Simons WJF, Socquet A, Vigny C, Ambrosius BAC, Haji Abu S, Promthong C, Subarya C, Sarsito DA, Matheussen S, Morgan P, Spakman W (2007) A decade of GPS in Southeast Asia: Resolving Sundaland motion and boundaries. J Geophys Res: Solid Earth (1978–2012) 112(B6):1

Wessel P, Smith WHF (1998) New, improved version of the generic mapping tools released. EOS Trans AGU 79(47):579